# Figure S1

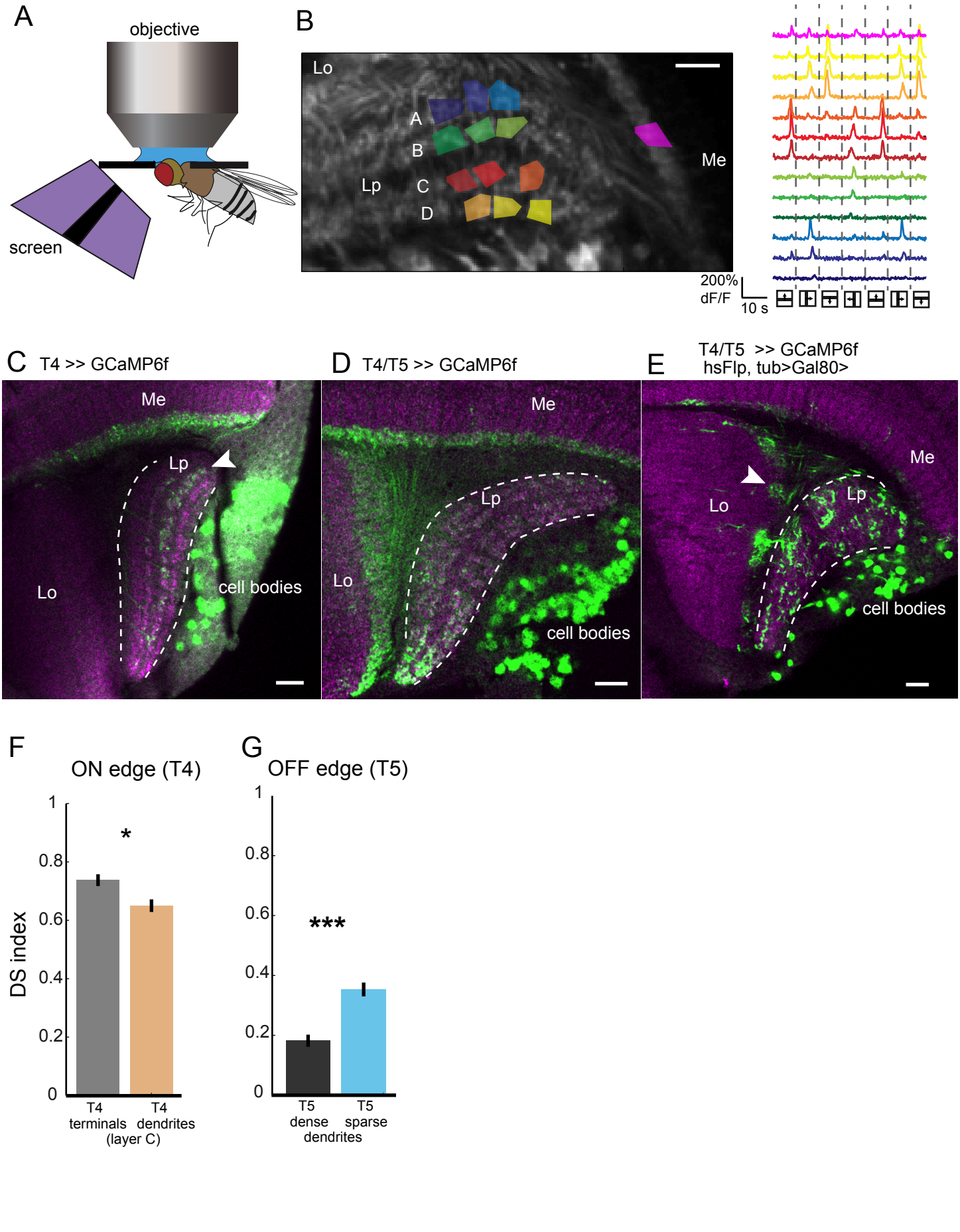
A
objective
screen
B
Lo
A
B
C
D
Lp
Me
200%
dF/F
10 s
C T4 >> GCaMP6f
Me
Lp
Lo
cell bodies
D T4/T5 >> GCaMP6f
Me
Lp
Lo
cell bodies
E T4/T5 >> GCaMP6f
hsFlp, tub>Gal80>
Me
Lo
Lp
cell bodies
F
ON edge (T4)
DS index
1
0.8
0.6
0.4
0.2
0
*
T4 terminals (layer C)
T4 dendrites
G
OFF edge (T5)
1
0.8
0.6
0.4
0.2
0
***
T5 dense dendrites
T5 sparse

# Figure S2

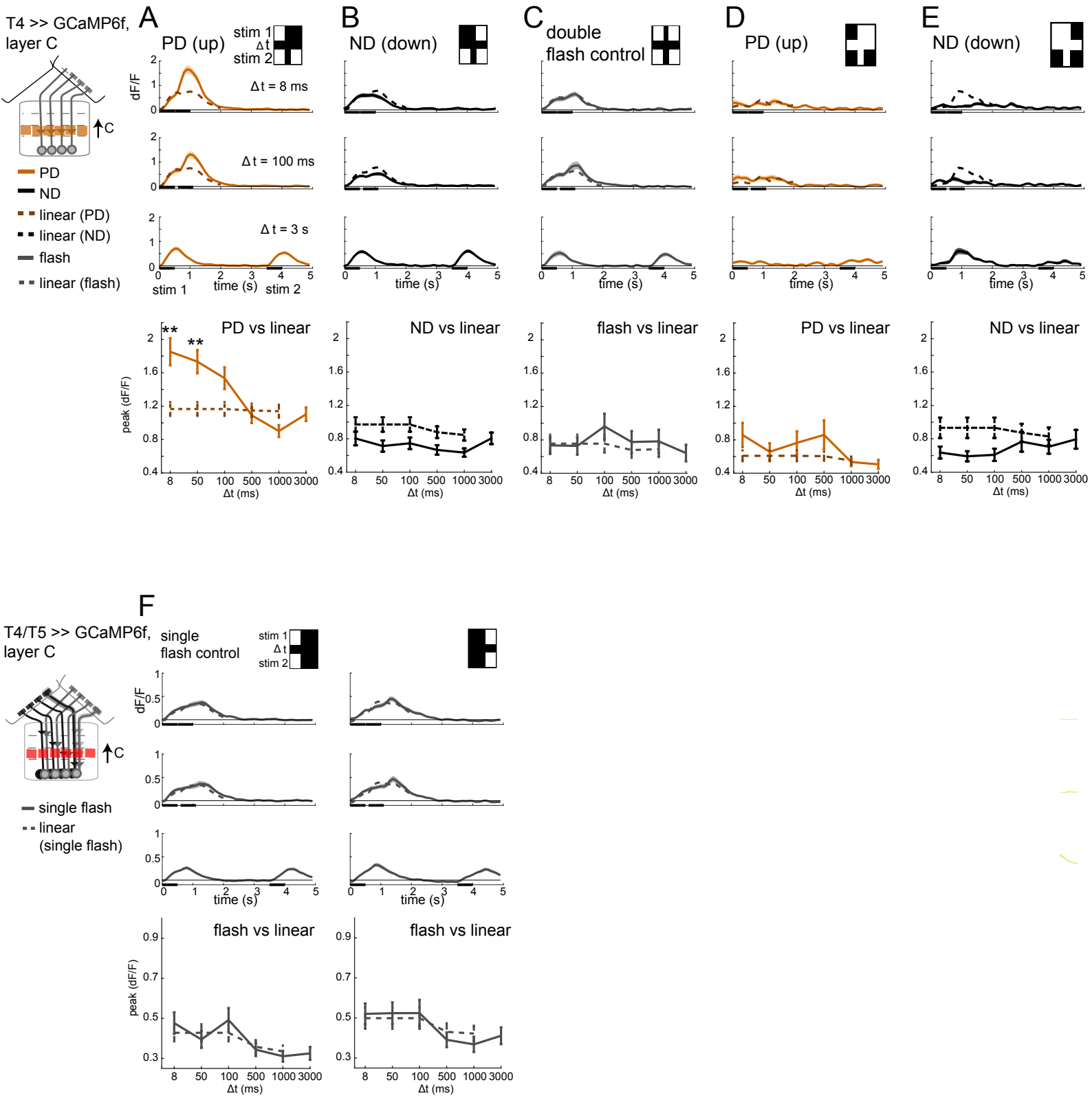
T4 >> GCaMP6f, layer C
C
PD
ND
linear (PD)
linear (ND)
flash
linear (flash)
A
PD (up)
stim 1
Δt
stim 2
dF/F
Δt = 8 ms
Δt = 100 ms
Δt = 3 s
stim 1
time (s)
stim 2
B
ND (down)
C
double flash control
D
PD (up)
E
ND (down)
PD vs linear
ND vs linear
flash vs linear
PD vs linear
ND vs linear
peak (dF/F)
**
**
Δt (ms)
F
T4/T5 >> GCaMP6f, layer C
single flash control
single flash
linear (single flash)
flash vs linear
flash vs linear

# Figure S3

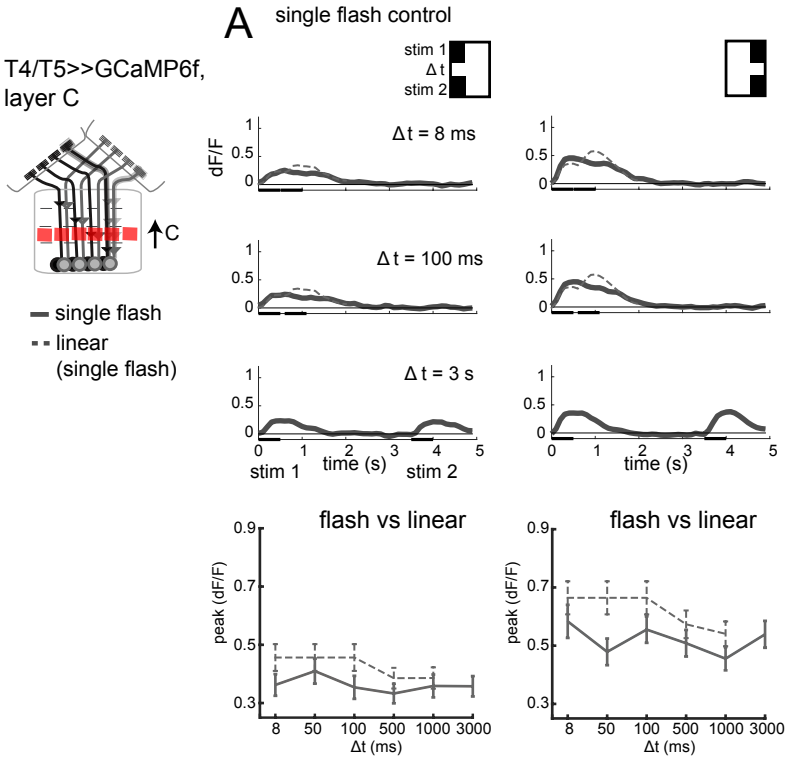
A
single flash control
T4/T5>>GCaMP6f,
layer C
C
single flash
linear
(single flash)
stim 1
Δt
stim 2
dF/F
Δt = 8 ms
Δt = 100 ms
Δt = 3 s
time (s)
stim 1
stim 2
flash vs linear
peak (dF/F)
Δt (ms)
8 50 100 500 1000 3000

# Figure S4

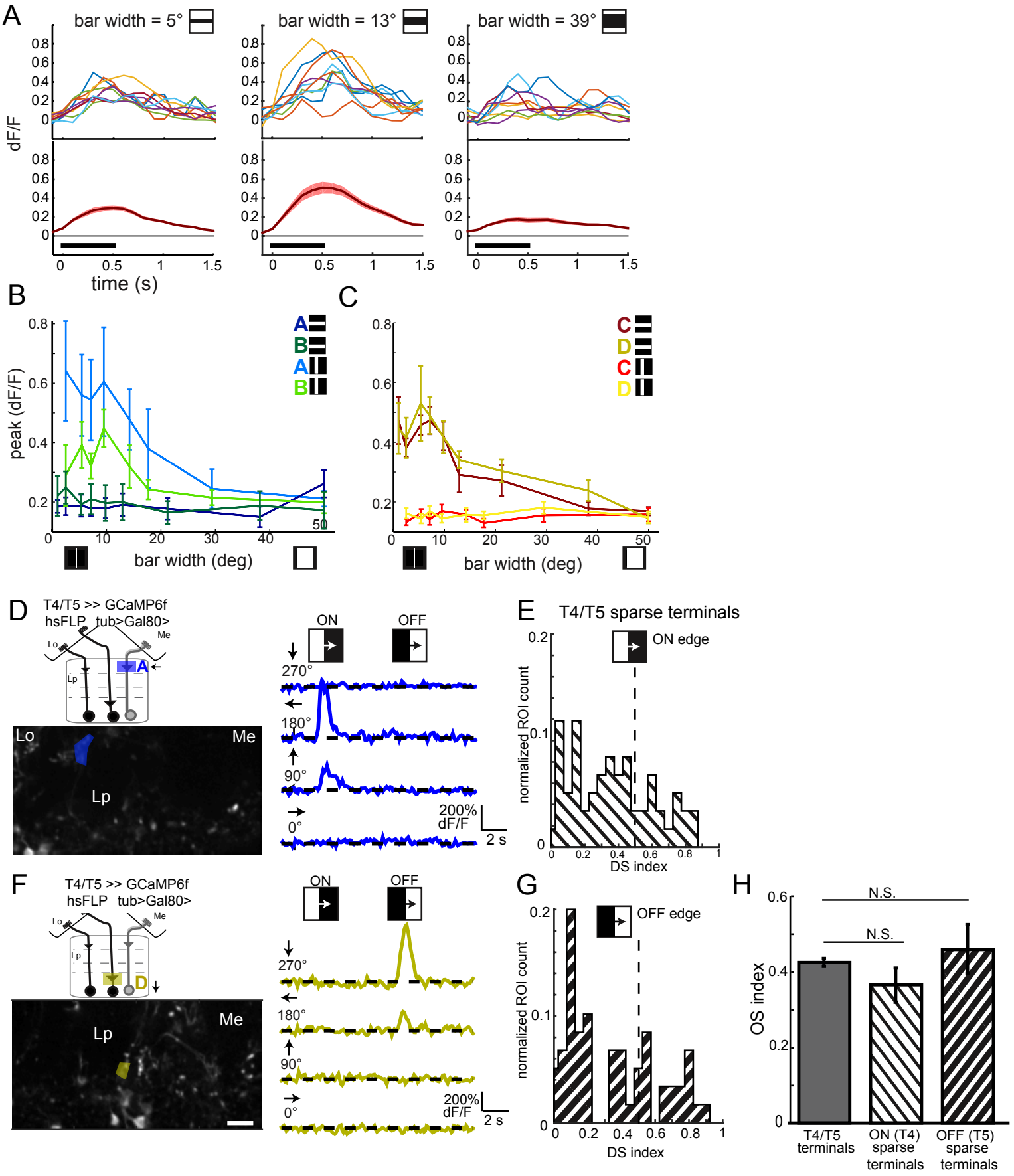
A
bar width = 5°
bar width = 13°
bar width = 39°
dF/F
time (s)
B
peak (dF/F)
bar width (deg)
C
bar width (deg)
D
T4/T5 >> GCaMP6f
hsFLP tub>Gal80>
Lo
Me
Lp
ON
OFF
270°
180°
90°
0°
200% dF/F
2 s
E
T4/T5 sparse terminals
ON edge
normalized ROI count
DS index
F
T4/T5 >> GCaMP6f
hsFLP tub>Gal80>
G
OFF edge
H
N.S.
OS index
T4/T5 terminals
ON (T4) sparse terminals
OFF (T5) sparse terminals

# Figure S5

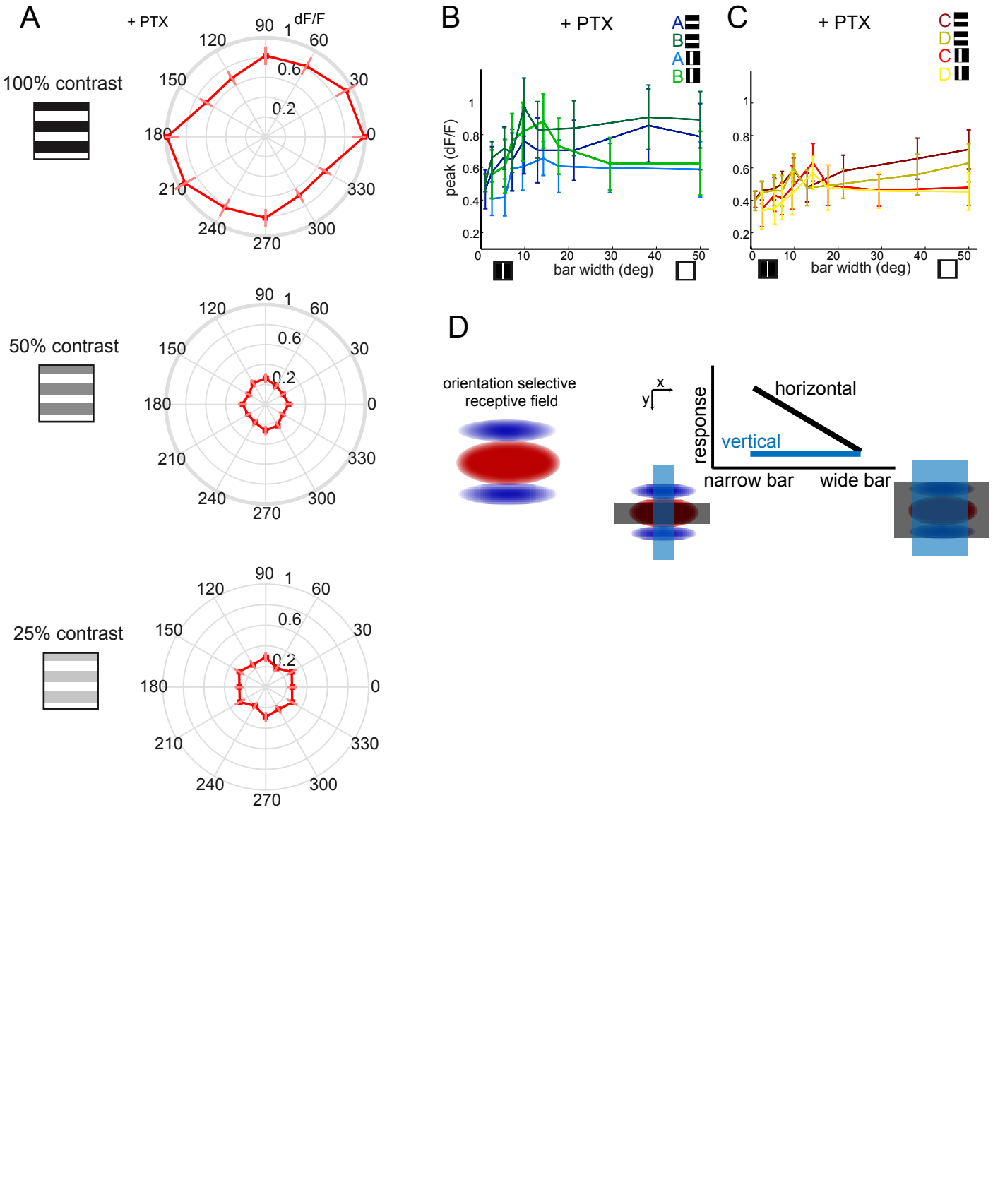
A
+ PTX
dF/F
100% contrast
50% contrast
25% contrast
90
120
60
150
30
180
0
210
330
240
300
270
1
0.6
0.2
B
+ PTX
A
B
A
B
peak (dF/F)
bar width (deg)
C
+ PTX
C
D
C
D
bar width (deg)
D
orientation selective
receptive field
x
y
response
horizontal
vertical
narrow bar
wide bar

# Figure S6

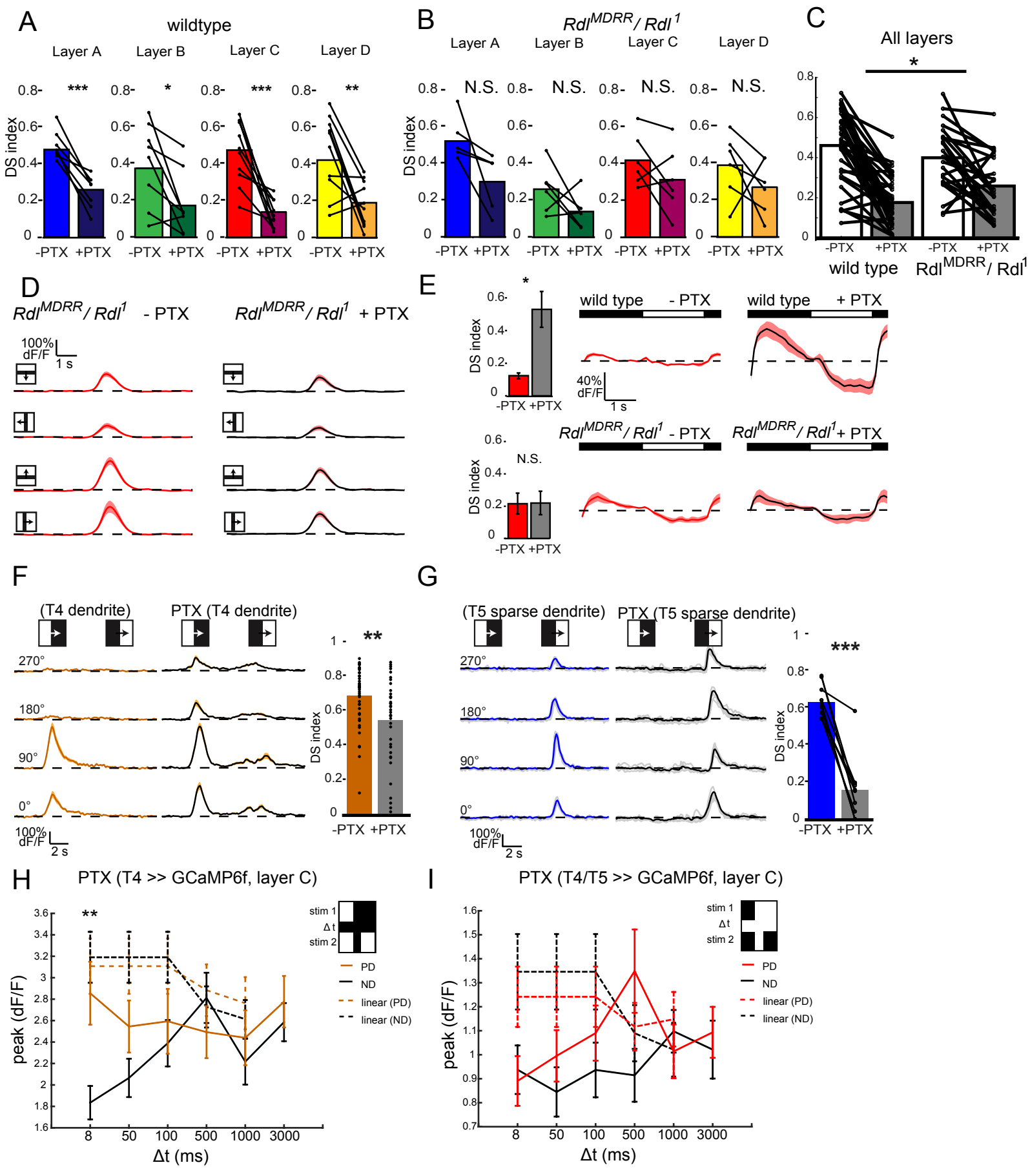
A
wildtype
Layer A
Layer B
Layer C
Layer D
DS index
-PTX +PTX
B
Rdl^MDRR / Rdl^1
N.S.
C
All layers
wild type
Rdl^MDRR / Rdl^1
D
Rdl^MDRR / Rdl^1 - PTX
Rdl^MDRR / Rdl^1 + PTX
100% dF/F
1 s
E
wild type - PTX
wild type + PTX
40% dF/F
F
(T4 dendrite)
PTX (T4 dendrite)
270°
180°
90°
0°
2 s
G
(T5 sparse dendrite)
PTX (T5 sparse dendrite)
H
PTX (T4 >> GCaMP6f, layer C)
peak (dF/F)
Δt (ms)
stim 1
Δt
stim 2
PD
ND
linear (PD)
linear (ND)
I
PTX (T4/T5 >> GCaMP6f, layer C)

# Figure S7

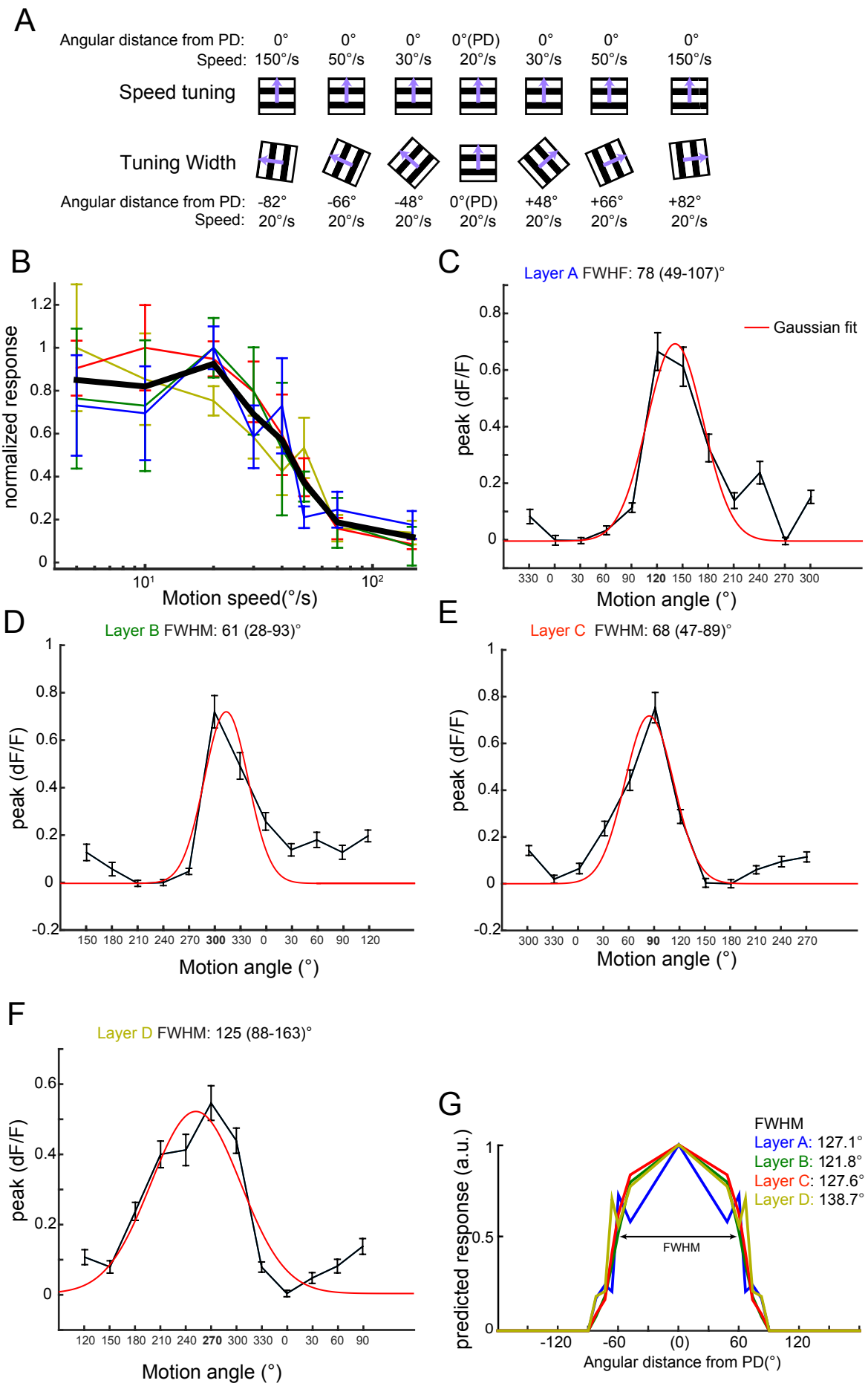
A
Angular distance from PD: 0° 0° 0° 0°(PD) 0° 0° 0°
Speed: 150°/s 50°/s 30°/s 20°/s 30°/s 50°/s 150°/s
Speed tuning
Tuning Width
Angular distance from PD: -82° -66° -48° 0°(PD) +48° +66° +82°
Speed: 20°/s 20°/s 20°/s 20°/s 20°/s 20°/s 20°/s
B
normalized response
Motion speed(°/s)
C
Layer A FWHF: 78 (49-107)°
Gaussian fit
peak (dF/F)
Motion angle (°)
D
Layer B FWHM: 61 (28-93)°
peak (dF/F)
Motion angle (°)
E
Layer C FWHM: 68 (47-89)°
peak (dF/F)
Motion angle (°)
F
Layer D FWHM: 125 (88-163)°
peak (dF/F)
Motion angle (°)
G
FWHM
Layer A: 127.1°
Layer B: 121.8°
Layer C: 127.6°
Layer D: 138.7°
FWHM
predicted response (a.u.)
Angular distance from PD(°)

**SUPPLEMENTAL INFORMATION**

**SUPPLEMENTAL FIGURE LEGENDS**

**Figure S1. Imaging T4 and T5 axon terminals and dendrites. Related to Figure 1.**

**(A)** Schematic of *in vivo* calcium imaging set-up. **(B)** Example maximum intensity projection of a time series, imaged in T4 and T5 axon terminals expressing GCaMP6f. Example ROIs are drawn, with layer specific color coding for the four lobula plate layers (A = blue, B = green, C = red, D = yellow). *In vivo* calcium imaging raw traces for the highlighted ROIs are shown, responding to a dark bar moving in four directions. **(C – E)** Maximum intensity projection confocal images of brains stained with anti-GFP (green) and nc82 (magenta), showing expression patterns of the genotypes used for calcium imaging. Brain regions are indicated as Me = medulla, Lo = lobula, Lp = lobula plate. Arrowheads indicate the selective GCaMP6f expression in lobula plate layer C **(C)** and a dendrite in a sparse T5 clone in the lobula **(E)**. Scale bar is 15 μm in **(B)** and 10 μm in **(C - E)**. **(F, G)** Quantification of direction selectivity using a DS index. Sample sizes (N = number of flies (ROIs)) are N = 12 (117) T4 terminals in lobula plate layer C and N = 13 (74) T4 dendrite ROIs **(F)** and N = 13 (84) T5 sparse dendrites and N = 6 (37) for T5 dense dendrites **(G)**. * $p<0.05$, *** $p<0.001$, two tailed Student's t-test.

**Figure S2. T4 responses to apparent motion stimuli. Related to Figure 2.**

Calcium signals imaged in the axon terminals in response to apparent motion and flash control stimuli. Average responses of three different temporal delays (Δt = 8 ms, 100 ms, 3 s) are shown above. Quantification of the measured peak calcium response at all 6 temporal time delays are compared with a linear prediction (dotted line) that is based on the separated responses recorded at Δt = 3 s are shown below. **(A-B)** Calcium signals imaged in the axon terminals of T4 in lobula plate layer C in response to the bright bar apparent motion stimulus, N = 10(64). **(C)** Calcium signals imaged in the axon terminals of T4 in lobula plate layer C in response to the bright bar flash control stimulus, N = 4(17). **(D-E)** Calcium signals imaged in the axon terminals of T4 in lobula plate layer C in response to the dark bar apparent motion stimulus, N = 6(19). **(F)** Calcium signals imaged in the axon terminals of T4 and T5 in lobula plate layer C in response to the bright bar single flash control stimulus N = 8(26). ** $p<0.01$, unpaired two tailed Student's t-test with Bonferroni correction for multiple comparisons. Inset shows X-T plots of the stimulus used in each experiment. Appropriate DS responses were also obtained from layers A, B and D using the apparent motion stimuli. However, unfavorable orientation or position within the brain made it difficult to consistently and reliably measure such signals within these layers. These layers were excluded from the analysis of linearity.

**Figure S3. T4 responses to flash control stimuli. Related to Figure 3.**

**(A)** Calcium signals imaged in the axon terminals of T4 and T5 in lobula plate layer C in response to the dark bar single flash control stimulus N = 9(37). $p>0.05$ for all

data, unpaired two tailed Student's t-test with Bonferroni correction for multiple comparisons. Inset shows X-T plots of the stimulus used in each experiment.

**Figure S4. T4 and T5 responses to static stimuli are orientation tuned and exhibit surround antagonism. Related to Figure 4.**

**(A)** Calcium responses to horizontally oriented dark bars of 3 different widths. Raw traces from 10 example ROIs are displayed above and average traces from all ROIs recorded in lobula plate layer C are shown below, N = 7(56). The black bar below the average trace shows when the bar was presented on the screen. Shaded regions reflect ±SEM. **(B, C)** Peak calcium responses to horizontally or vertically oriented light bars of different widths, imaged in T4 and T5 axon terminals in the lobula plate. Sample sizes are N = 5 (7) in layer A and N = 4 (5) in layer B **(B).** N = 6 (17) in layer C, N = 6 (17) in layer D **(C)**. **(D)** Example T4 clone that is specific for moving ON edges and is a putative layer A terminal based on its directional preference for 180° (OS tuning for this example clone is shown in Figure 4F). A single region of interest (ROI) that was analyzed to extract the traces shown below is shaded in blue. Traces display calcium responses of this example T4 clone to moving ON and OFF edges. **(E)** Normalized histogram displaying the direction selectivity using a DS index for moving ON edges for ROIs from T4/T5 stochastic clones, N = 5(59). **(F)** Example T5 clone that is specific for moving OFF edges and is a putative layer D terminal based on its directional preference for 270° (OS tuning for this example clone is shown in Figure 4H). The single ROI that was analyzed to extract the traces shown below is shaded in yellow. Traces display calcium responses of this example

T5 clone to moving ON and OFF edges. **(G)** Normalized histogram displaying the direction selectivity using a DS index for moving OFF edges for ROIs from T4/T5 stochastic clones, N = 5(59). **(H)** Bar plot showing the average OS indices for ROIs from different genotypes. Sample sizes are N=9(458) dense T4/T5 axon terminals, N = 4(16) ON sparse terminals and N = 4(17) OFF sparse terminals. N.S. = not significant, two tailed Student's t-test. Error bars reflect ±SEM.

**Figure S5. Orientation selectivity and surround antagonism in T4 and T5 require inhibitory signaling. Related to Figure 5.**

**(A)** Polar plots displaying peak calcium responses in T4 and T5 axon terminals to static gratings of different orientations at 100%, 50% and 25% contrast after application of picrotoxin (PTX). **(B, C)** Peak calcium responses to horizontally or vertically oriented light bars of variable width, imaged in T4 and T5 axon terminals in the lobula plate after application of PTX. Sample sizes are N = 3 (10) in layer A and N = 3 (13) in layer B **(B)** and N = 3 (18) in layer C, N = 3 (14) in layer D **(C). (D)** Schematic displaying how a receptive field containing elongated excitatory (red) and inhibitory (blue) sub-regions could create both orientation selectivity and an antagonistic surround.

**Figure S6. Directionally tuned responses in T4 and T5 require inhibitory signaling. Related to Figure 6.**

**(A)** Bar plots quantify the responses to moving bars of 100% contrast of all lobula plate layers, before and after PTX application, N = 10 flies, paired Student's t-test, *

p<0.05, ** p<0.01 and *** p<0.001. **(B)** Bar plots quantify the responses shown in **(D)**, as well as the equivalent responses in all other layers of the lobula plate in $Rdl^{MDRR}$ / $Rdl^{1}$ mutants, before and after PTX application, N = 5 flies (layer A) and N = 6 flies (layers B, C, D), paired Student's t-test, N.S. = not significant. **(C)** Responses before and after PTX treatment, in wild type and $Rdl^{MDRR}$ / $Rdl^{1}$ mutants, pooled across the four layers. Asterisk denotes that there is a significant difference between the means of the genotypes after treatment (Two-way Anova $F(1, 56) = 4.96$, $p < 0.05$) but not before treatment (Two-way Anova $F(1, 56) = 1.70$, $p > 0.05$). **(D)** Responses to moving dark bars in mutant flies carrying the PTX-insensitive allele $Rdl^{MDRR}$ in trans to the *Rdl* null allele $Rdl^{1}$. **(E)** Calcium response traces to a full field light flash of 100% contrast, changing contrast every 2 s. Wild type responses are shown at the top, responses in $Rdl^{MDRR}$ / $Rdl^{1}$ mutants at the bottom, both measured in T4 and T5 axon terminals in lobula plate layer C. Mean traces of N = 5 (18) and N = 6 (10) wild-type flies before and after PTX application, and N = 3 (10) and N = 4 (10) *Rdl* mutant flies before and after PTX application, shading denotes ±SEM. **(F)** Traces displaying *in vivo* calcium responses of T4 dendrites to moving ON and OFF edges (stimulus schematic on top). Shown is the mean trace of N = 8 (44) flies (ROIs) before and N = 5 (38) after PTX application. Bar plots quantify the DS index. ** p<0.01 two-tailed Student's t-test. **(G)** Traces displaying *in vivo* calcium responses of a sparsely labeled T5 dendrite to moving ON and OFF edges. Shown is the mean response to repeated stimulus presentations of this single ROI. DS index of this individual ROI was 0.55 before and 0.04 after PTX application. The bar plot shows the quantification of N = 10 paired ROIs pre- and post PTX treatment, N =

7(10), *** p<0.001, paired Student's t-test. **(H)** Quantification of the peak calcium response at various time delays, comparing PD and ND responses in T4, lobula plate layer C, for light bars upon PTX application, ND observations at 8 and 50ms are non-linear. N = 4 (20). ** p<0.01, unpaired two tailed Student's t-test with Bonferroni correction for multiple comparisons. **(I)** Quantification of the peak calcium response at various time delays, comparing PD and ND responses in T4 and T5 lobula plate layer C, for dark bars upon application of PTX. N = 7 (28). No data points are significantly different, two tailed Student's t-test. Inset shows X-T plots of the apparent motion stimulus.

**Figure S7. Directionally tuned responses in T4 and T5 are narrower than speed tuning would predict. Related to Figure 7.**

**(A)** Schematic description of the stimuli used to measure the speed tuning values used for the tuning width prediction (top), and the corresponding stimuli used to measure true directional tuning width (bottom). **(B)** Responses of T4 and T5 to square-wave gratings moving at different speeds. For each layer in the lobula plate, responses were measured at the preferred direction for that layer and normalized to the maximum response at a given speed. The average speed tuning across all four layers is plotted in black with individual layers shown in color, error bars denote ±SEM. Layer A: N = 3-14(11-108); Layer B: N = 3-15(12-106); Layer C: N = 3-15(16-135), and Layer D: N = 3-15(13-109). **(C - F)** Measured directional tuning curves (black lines) of T4 and T5 axon terminals of layer A-D were fit by Gaussian functions

(red lines) to determine the full width at half maximum (FWHM). **(G)** The predicted tuning width is reproduced from Figure 7 for comparison.

## SUPPLEMENTAL EXPERIMENTAL PROCEDURES

### CALCIUM IMAGING

#### Fly preparation and imaging set-up

Flies were grown on molasses-based food on a 12:12 hour light:dark cycle at 25°C and imaged at room temperature (20°C). Female flies of all genotypes were imaged within 24 hours of eclosion and immobilized on ice for mounting into the microscope holder. *In vivo* 2-photon calcium imaging experiments were performed as in Silies et al. (2013) and Clark et al. (2011). A visual stimulus was produced using a digital light projector (DLP) with a frame rate of 240Hz that projected onto a 8 cm x 8 cm rear-projection screen positioned anterior to the fly. The following additional modifications were made to this set up: The excitation wavelength for GCaMP6f was 920 nm. Emitted light was sent through a SP680 short pass filter and a 560 dichroic filter before entering a 525/50 emission filter (Semrock, Rochester, NY). This allowed presentation of visual stimuli through a 448/20 bandpass filter and a ND0.5 neutral density filter without it being detected by the microscope PMTs. The screen spanned 80° of the fly's visual field horizontally and 50° vertically. The overall luminance of the screen was 0.03 Watts /$m^2$/sr. Contrast values are given as Michelson contrast. All data were acquired at a constant frame rate of 5.6 Hz using frame sizes of 200*100 pixels and a line scan rate of 700 Hz in unidirectional scanning mode.

#### Visual stimuli

All of the visual stimuli presented contained epochs where aspects of the stimulus parameters change (e.g. motion direction, grating orientation, delay between bar presentations). For example an experiment in which a bar is presented that is moving in one out of eight different directions, we would call this one stimulus with eight epochs. The order of these epochs was randomly defined at the beginning of any stimulus presentation. However, if a single stimulus presentation was long enough to repeat the epochs, the chosen order was maintained. In this

manner, data was collected containing responses to each epoch a similar number of times, but each new brain region or new fly was presented with a distinct stimulus order to control for potential effects of timing between the different epoch trials.

Moving dark bar

An approximately 8° wide dark bar was moved at 20°/s across a bright screen at 100% contrast. Eight directions were presented: a vertical bar moving left or right across the horizontal extent of the screen, a horizontal bar moving up or down across the vertical extent of the screen or bars moving in both directions along the two diagonals. There was a 4.5 s gap between bar presentations to allow responses to decay to baseline. The stimulus was generally repeated so as to allow the bar to pass the screen at least 19 times. In a variation of this stimulus, the bar was displayed at 100%, 50% or 25% contrast, moving in four directions (a vertical bar moving left or right across the horizontal extent of the screen or a horizontal bar moving up or down across the vertical extent of the screen).

Moving edge stimulus

A light (ON) edge that moved across the screen at 20°/s with 100% contrast was used. After the bright edge swept across the screen, leaving the full screen illuminated for ~5 s, a dark (OFF) edge moving in the same direction at 20°/s was presented. Four motion directions were presented: vertical edges moving left or right across the horizontal extent of the screen, or horizontal edges moving up or down across the vertical extent of the screen. The stimulus was generally presented long enough to allow the bar to pass the screen at least 5 times, but longer recordings were used to capture responses from single ROIs (Figure 1).

Apparent motion stimuli

To produce an apparent motion stimulus, a 3° wide bar was presented for 0.5 seconds (stim1), disappeared for a variable time, and was then followed by a pair of bars (stim 2), one positioned at the original position and one offset by 2° in visual space. The temporal delay varied between presentations and was 8 ms, 50 ms, 100

ms, 500 ms, 1 s or 3 s long. To generate the double flash control stimulus, both stim1 and stim2 were presentations of a pair of bars, separated by the same temporal delays described above. To generate the single flash control stimulus both stim1 and stim2 were presentations of a single bar displayed sequentially at the same location, either the first or second location used for the apparent motion stimulus, depending on which rendition of the single flash control was being shown. Both dark and bright bars were used, and were presented at full contrast. Since these stimuli only occupy a small part of visual space, a responding brain region was always identified first by presenting dark moving bars and visually inspecting the lobula plate for calcium responses.

Static bars of different widths

A static bar of 100% contrast was displayed for 0.5 seconds, with 2 seconds between bar presentations. The width of the presented bars ranged from 2.5° to 50° horizontally (for a vertical bar spanning the screen from top to bottom) and 1° to 50° vertically (for a horizontal bar spanning the full screen from left to right). Peak dF/F values were used for quantification.

Full Field Flash Stimulus

Periodic presentation of light flashes lasting 2 s were interleaved with 2 s of darkness. The stimulus was typically presented for approximately 40 s or 400 imaging frames, such that at least 8 flashes of light were presented.

Static and Moving Grating Stimulus

The stimulus began with a static presentation of a square-wave grating oriented in one of 12 directions that lasted 1.5 seconds. The grating was displayed at full contrast and had a spatial period of 20°. Next, the grating moved at a constant velocity orthogonal to the orientation of the grating for 2 seconds. The grating speeds used were 5°/s, 10°/s, 20°/s, 30°/s, 40°/s, 50°/s, 70°/s and 150°/s. A gray display was interleaved for 1.5 seconds between each grating epoch.

**Data analysis**

The average intensity within each region of interest (ROI) was computed for each frame to generate a time-trace of the response as a function of time. ROIs were manually drawn and assigned either to one of the four lobula plate layers or to a dendritic region within the medulla (T4) or lobula (T5) by visual inspection. All responses and time-traces of stimuli were interpolated to 10 Hz prior to averaging. In order to remove slow fluctuations of the baseline fluorescence that could occur over the course of a long stimulus presentation, a $4^{th}$ order polynomial was fit to the response trace of each ROI over the full duration of a block of stimulus epochs. This $4^{th}$ order polynomial was then subtracted from the measured trace. Receptive field centers of each ROI were determined as described in Freifeld et al. 2013, using responses to dark moving bars on a bright background. Receptive field center coordinates of ROIs imaged while displaying other stimuli were then matched based on z-depth and manual assignment.

For each ROI, the mean response to each epoch was computed whenever multiple stimulus presentations occurred within a time trace. For the majority of imaging experiments, these mean ROI responses were averaged together across all similar ROIs for a particular neuronal subtype (e.g. Layer A) or neuronal compartment (e.g. Layer C T4 dendrite region in the medulla).

However, for experiments that assessed the response of particular layers within the lobula plate to a full field flash, moving bar response or moving edges stimuli before and after the application of PTX, the mean response across ROIs of a particular layer was calculated and then an average was taken between the mean responses for each individual fly. This mean fly trace allowed a paired comparison of the effect of the drug treatment on response properties without having to align ROIs before and after application of the drug (Figure 6, Figure S6A-E). For the assessment of the effect of PTX on the response properties of T4 or T5 dendrites the analysis was performed based on single ROI response properties and in the case of T5 dendrites single ROIs were aligned before and after the drug treatment to allow a paired comparison of single T5 dendrites (Figure S6F,G).

Analysis of apparent motion stimuli

Analysis was restricted to cells that (i) have a receptive field center and thus directly see the screen and (ii) showed visible responses in the raw response traces to the apparent motion presentation with Δt = 3s, to either stim1,stim2, for the PD or ND bar presentation. The linear prediction was calculated using the individual responses to stim 1 and stim 2 at Δt = 3s. Mean response traces from stim 1 and stim 2 were obtained and shifted in time to match the timing produced by the variable Δt value for each individual epoch. The traces were then summed together.

Analysis of moving bar responses

Response traces of individual ROIs were first coarsely aligned using the position of the receptive field center. Alignment was then refined by shifting different time-traces by the delay that brought the cross-correlation between the specific trace and the mean trace to a maximal value, where the maximum shift allowed was 50 frames. DS indices were then calculated by assigning the preferred direction (PD) to the bar motion that elicited the maximum response and the null direction to the direction that was 180° offset to the PD. Peak dF/F values were then used to calculate DS indices as

$$DS_{index} = \frac{(PD - ND)}{(PD + ND)}$$

Tuning curves (polar plots) were calculated from all ROIs that were assigned to have a moving bar response in at least one of the eight directions. From these ROIs, fly means for each layer were calculated and response values for the eight motion directions were obtained by integrating under the response curve. To reduce the impact of noise from baseline fluorescence fluctuations, we measured the standard deviation of the trace from a portion of the trace preceding any stimulus (to get a measure of its noise). Two standard deviations above the baseline was set as a threshold and any values below that cut off were set to zero. We then integrated under the remaining curve.

For paired comparisons before and after PTX treatment, ROIs were matched for individual flies that were first imaged without PTX and then imaged after PTX application.

Analysis of moving edge responses

Response traces of individual ROIs were aligned by the position of the receptive field center. DS indices were calculated as described above for the moving bar analysis, using separate peak dF/F values for the ON edge response period (0 - 8 s) and the OFF edge response period (10 – 23.9 s).

Analysis of OS and DS tuning in response to static and moving grating stimuli

Analysis was restricted to ROIs that had a measurable receptive field center in response to the moving bar stimulus. Mean traces reflect an average of all ROI responses. To calculate the orientation and directional tuning width, the mean dF/F response for each ROI was found during each epoch, for both the static period (to measure orientation tuning) and the motion period (to measure direction tuning). These mean dF/F responses were used to produce the polar plots that display orientation selectivity and direction selectivity for grating stimuli in Figure 4, 5 and 7.

Analysis of the angle $\theta$ between the OS and DS axis

To calculate the angle between OS and DS axis for each ROI, first a summed vector response was used to calculate the angle of the preferred direction and angle of the preferred orientation. The preferred direction (DS) vector was calculated using the responses to all 12 directions of a moving grating for each of the individual ROIs. Each data point was treated as vectors ( $\theta_{nDS}$, $R_{nDS}$). In which $\theta_{nDS}$ is the direction of grating movement for the $n^{th}$ direction epoch and $R_{nDS}$ is the dF/F response observed for that epoch. Using this vector data we calculate $\theta_{vPD}$ and $V_{PD}$.

$$\theta_{vPD} = \tan^{-1}\left(\frac{\sum_n R_{nDS}\sin(\theta_{nDS})}{\sum_n R_{nDS}\cos(\theta_{nDS})}\right)$$

$$V_{PD} = \sqrt{\left(\sum_n R_{nDS}\cos(\theta_{nDS})\right)^2 + \left(\sum_n R_{nDS}\sin(\theta_{nDS})\right)^2}$$

Where $\theta_{vPD}$ was the angle of the summed response vector that is used as the preferred direction angle (PD) and $V_{PD}$ is the length of the summed response vector (dF/F).

To calculate the preferred orientation (OS) vector, the responses to all 12 directions of the static grating for each of the individual ROIs were measured. This array of 12 measurements was shifted such that the maximum response was at the 4$^{th}$ index. Then the 1$^{st}$-6$^{th}$ measurements were averaged with 7$^{th}$-12$^{th}$ measurements since they represent duplicate data obtained using a static grating of the same orientation. From this we obtained 6 data points that can each be treated as vectors ( $\theta_{nOS}$, $R_{nOS}$) in which $\theta_{nOS}$ is the orientation of static grating for the n$^{th}$ direction epoch and $R_{nOS}$ is the dF/F response observed for that orientation of grating. Using this vector data we calculate $\theta_{vPO}$.

$$\theta_{vPO} = \tan^{-1}\left(\frac{\sum_n R_{nOS}\sin(\theta_{nOS})}{\sum_n R_{nOS}\cos(\theta_{nOS})}\right)$$

Where $\theta_{vPO}$ as the angle of the summed response vector that is used as the preferred orientation angle (PO).

Then, to solve for the angle between the preferred DS and OS $\theta$ axis for each ROI

$\theta_{vPO}$ was subtracted from $\theta_{vPD}$. To avoid noisy and thus arbitrary DS and OS measurements that might arise from weakly responding ROIs, Only ROIs with a preferred direction vector ($\underline{V_{PD}}$) greater than 50% dF/F were reported for this analysis (Figure 7F).

Quantification of tuning width

The average response to each direction of a moving grating with a 20° spatial period moving at a constant velocity of 20°/s, was measured for each layer within the lobula plate. To subtract baseline activity, the smallest direction response was subtracted from all of the measured responses to produce the curves displayed in Figure S7. Next these population-tuning curves were fit with a Gaussian function

$$F(x) = ae^{\left(-\left(\frac{x-b}{c}\right)\right)^2}$$

where x is the angle of the motion stimulus (°), F(x) is the measured response value, a = $1/(\sigma*\mathrm{sqrt}(2\pi))$ sets the height of the curve's peak, b = μ sets the position of the center of the peak, and c= sqrt(2)*σ relates to the width of the curve; $\sigma^2$ = variance and μ= expected value.
Using this function, the full width at half maximum (FWHM) was calculated as:

$$FWHM = 2\sqrt{\ln(2)}\ c$$

Fitted Gaussian functions for different layers were normalized and the maximal response was shifted to be the PD response in Figure 7H to allow a comparison of this measured tuning width with predicted tuning widths.

Analysis of predicted tuning width

An elementary motion detector analyzes motion along its PD-ND axis. Thus, a motion stimulus that is rotated with respect to this axis hits the two inputs of the correlator (Figure 7G) at an apparent speed that is faster than the actual forward

movement of the stimulus. We utilized this difference to predict responses to moving stimuli that are rotated with respect to the PD-ND axis. Specifically, a grating that is rotated relative to this PD-ND axis will appear to the motion correlator to move at a faster speed. If the assumption of a one-dimensional motion detector is correct, then the manner in which speed tuning and width tuning decay from their optimal stimulus (speed or direction) should be related by this underlying geometry. Thus, we calculated the ratio between the measured responses at the optimal grating speed (20°/s) moving in the preferred direction to responses of gratings moving at 30°/s, 40°/s, 50°/s 70°/s and 150°/s in the same preferred direction. These ratios were used to predict the response to a grating moving at 20°/s tilted away from the PD-ND axis by ~48°, 60°, 66°, 73° and 82° respectively. The PD was defined as the orientation that resulted in the biggest response in the directional tuning analysis (Figure 7E). A grating with orthogonal orientation (90°) to the PD-ND axis does not generate a motion response and was thus set to 0.

**Genetics**

The following genotypes were used in this study:

T4/T5 imaging:

$w^+$ *; UAS-GCaMP6f / + ;* $T4/T5^{GMR42F06}Gal4^{attP2}$ */ +*

T4 lobula plate layer C subtype imaging

$w^+$ *; UAS-GCaMP6f / + ;* $T4^{GMR54A03}Gal4^{attP2}$ */ +*

Stochastic T4/T5 imaging:

$w^+$ */ hsFlp ; UAS-GCaMP6f / tub-FRT-Gal80-FRT ;* $T4/T5^{GMR42F06}Gal4^{attP2}$ */ +*

To create stochastic T4 and T5 labeling, a brief heat-shock was applied during larval development to induce expression of Flippase, which stochastically removed Gal80 from the FLP-out cassette. The removal of Gal80 repression thereby allows Gal4 to express GCaMP6f in a random subset of T4 and T5 neurons (Figure 1D and Figure S1E).

PTX insensitive *Rdl* background:

$w^{+}$ ; *UAS-GCaMP6f* / + ; *T4/T5*$^{GMR42F06}$*Gal4*$^{attP2}$ , *Rdl*$^{1}$/ *Rdl*$^{MDRR}$

**Pharmacology**

The $GABA_AR$ antagonist picrotoxin was dissolved in water and applied at a concentration of 5 μM in saline, prepared from a 50 mM stock solution. Flies were first imaged without PTX to obtain control data. The PTX-containing solution was then allowed to replace the saline over a 10 min time period before the PTX condition was imaged.

**CONFOCAL IMAGING**

To image expression patterns, *Gal4* driver lines were crossed to *UAS-GCaMP6f*, and dissected, fixed, and stained with an anti-GFP antibody (chicken anti-GFP, Abcam, 1:2000) and anti-Bruchpilot (nc82, DSHB, 1:30) using standard methods. Brains were imaged using a Leica TCS SP8 confocal microscope (Bensheim, Germany) with 40x (NA = 1.25) lens. Confocal images were rendered in three dimensions using Imaris (Bitplane), adjusted using cropping and thresholding tools in Photoshop (Adobe), and assembled into figures using Illustrator (Adobe).